Available on CMS information server **CMS CR 1998/011**

CMS Conference Report

30 April 1998

TCAD-Based Analysis of Radiation-Hardness in Silicon Detectors

D. Passeri, M. Baroncini, P. Ciampolini

Istituto di Elettronica, Università di Perugia, Via Duranti 93, 06131 Perugia, Italy

G. M. Bilei, A. Santocchia, B. Checcucci, E. Fiandrini

INFN - Sezione di Perugia, Via A. Pascoli 1, 06100 Perugia, Italy

Abstract

The application of a general-purpose device-simulator to the analysis of silicon microstrip radiation detector is described. Physical models include charge-collection dynamics, as well as radiation-induced deep-level recombination centers. Realistic description of multiple-strip devices can be accounted for. To allow for validation of the analysis tool, actual detectors have been measured, before and after being irradiated with neutrons. Simulation predictions agree well with experiments. Limitations of the adopted model are discussed, with reference to simulation-based comparison with higher-order models.

Presented at *IEEE Nuclear Science Symposium*, Albuquerque (CA), November 14, 1997

To be published in *IEEE Transactions on Nuclear Science*, vol. 45, n. 3, June 1998

1 Introduction

Technology CAD (TCAD) tools are being extensively used for design and optimization of microelectronic devices. This allows for fast and inexpensive predictions of the device behavior, minimizing the need for prototype fabrication and making it possible to investigate sensitivity on different technological process parameters. Recently, by introducing suitable physical and mathematical models of transduction effects, such techniques have been progressively extended to the simulation of several classes of solid-state semiconductor sensors and transducers [1].

In particular, device simulation has been exploited for the analysis of solid-state, radiation-sensitive devices employed for high-energy physics, such as silicon microstrip detectors. Passive characterization of such devices was carried out [2] by straightforwardly applying standard simulation tools. Such efforts were mainly focused at investigating noise-related parameters, such as the leakage currents or parasitic capacitances. Dedicated programs have also been conceived [3, 4], aimed at the specific purpose of radiation detector simulation.

Such devices, in fact, although based on fairly simple operating principles, differ with many respects from VLSI ones. For this reason, in order to fully exploit the advantages offered by numerical analysis, conventional device-simulation programs (i.e., conceived for VLSI-device optimization) can hardly be directly employed and should be somewhat adapted to the peculiarity of such a particular context. Differences arise on a merely practical basis, as well as on more conceptual grounds. Among practical issues, it should be mentioned, for instance, a large difference in the range of involved physical dimensions and of applied voltages: actual detectors feature micrometric details, embedded in an active region which is two or three order of magnitude larger; large voltages are usually applied to deplete the device along its whole thickness. Discretization and solution algorithms actually need to be carefully tuned with respect to such kind of parameters.

More importantly, a set of additional physical mechanisms comes significantly into play: the detection mechanism itself, for instance, is usually based on the collection of charge generated by the ionising particles which cross the silicon layer. Active behavior of the detector (i.e., the actual particle detection) can thus be simulated only by accounting for such a phenomenon, which can instead be safely neglected in conventional device analysis.

With this respect, however, another topical issue concerns the “aging” of detectors, damaged by the continuing exposure to radiation at future, high-luminosity particle accelerators. Highly energetic particle hitting the device may induce the formation of bulk and surface recombination centers, as well as cause fixed-charge trapping at the insulating layers [5].

Under these circumstances, detector performance keeps degrading throughout its active life, which eventually results in setting severe limitations on both device reliability and sensitivity. Evaluating radiation-hardness at design-time therefore represents one of the key topics for the production of next-generation silicon detectors: updated CAD programs are therefore needed, providing the designer with radiation-aware analysis tools, useful in aiding both design and prototype testing phases.

In this work, we describe the application of a general-purpose device simulator to the analysis of silicon microstrip detectors: the HFIELDS program has been adopted to this purpose.

In order to make it suitable for particle-detector simulation, the code has then been customized with respect to some of the aforementioned, radiation-related issues. More explicitly, *i)*, a “dedicated” transient-analysis mode has been devised, which analyzes in detail the motion of a cloud of carriers generated by the particle hit, and, *ii)*, the simulation of arbitrarily “damaged” devices has been made possible by properly characterizing some of the transport equations terms.

In particular, contribution of deep-level recombination centers is accounted for and correlated to the radiation fluence; radiation-induced fixed charge trapped in the insulator layers and at interfaces is considered as well. Sect. 2 below gives some detail about features implemented into the code, and focuses on the customization of the program with respect to radiation effects.

It should be emphasized here that, from the physical standpoint, modeling of radiation damage is still largely an open question, and that a fairly wide spread of different (and sometimes contradictory) data can be found in the literature. We therefore tried to validate simulation results against experimental findings and, as illustrated in sect. 3, we were able to find a satisfactory agreement between simulated and measured data, even by using a relatively simple model, based on a single, deep-level trap. Nevertheless, there is physical evidence of some limitations connected to such a model, a qualitative discussion of which is carried out in sect. 3 itself, which includes a simulation-based comparison with a higher-order model.

Conclusions are eventually drawn in sect. 4.

2 The analysis method

Simulations have been performed by using a customized version of the HFIELDS code [6], originally developed at the University of Bologna. In the version adopted for this work, the program numerically solves the classical transport equations below:

$$\nabla\cdot(-\epsilon_s\,\nabla\varphi) = q(p - n + N) \tag{1}$$

$$\frac{\partial n}{\partial t} - \frac{1}{q}\nabla\cdot\vec{J}_n = (G-R)_{shallow} + (G-R)_{deep} + G_{track} \tag{2}$$

$$\frac{\partial p}{\partial t} + \frac{1}{q}\nabla\cdot\vec{J}_p = (G-R)_{shallow} + (G-R)_{deep} + G_{track} \tag{3}$$

Eq. 1 is the Poisson's equation, while Eqs. 2 and 3 are the carrier continuity equations for electrons and holes, respectively. Apart from details given in the following paragraphs, symbols have their usual meaning: φ is the electric potential, n and p are the electron and hole concentration, N_D and N_A stand for the donor and acceptor ion concentration, R and G indicate recombination and generation rates, respectively. Current densities $\vec{J}_n$ and $\vec{J}_p$ are expressed according to the Drift-Diffusion approximation:

$$\vec{J}_n = q\mu_n\left[-n\nabla\varphi + \frac{k_B T}{q}\nabla n\right] \tag{4}$$

$$\vec{J}_p = q\mu_p\left[-p\nabla\varphi - \frac{k_B T}{q}\nabla p\right] \tag{5}$$

Equations above are discretized on an almost arbitrary two-dimensional domain; most details concerning basic numerical algorithms and implementation issues can be found, for instance, in [6] (and references therein).

As introduced in the previous section, radiation issues enter the simulation operating mode with, at least, two different respects: charge collection and radiation damage.

2.1 Dynamic charge collection

Active detector response comes from the collection of carriers generated along the impinging particle track: as introduced in [7], the original code has been modified, to account for radiation-induced electron-hole pairs. Within the adopted model, a detailed, physical account is not actually needed neither for the primary collision events, nor for secondary impacts. Characterization of such mechanisms is known: for our purposes, we may assume that charge generation effects result in the rise of a charge "filament" having known density along the track. Furthermore, such a distribution develops in a timeframe which is much smaller than the actual collection time.

We therefore define an arbitrary spatial distribution of generated pairs following the hypothetical particle track; this results in the additional term:

$$G_{track} = G_{track}(x, y, t)$$

appearing in Eqs. 2 and 3. Starting from such a condition, a transient simulation accounts for the relaxation of the generated charge cloud: carriers travels within the semiconductor bulk under the combined action of electrostatic and diffusion forces. This permits an accurate reconstruction of actual charge trajectories, which in turn allows for predicting the shape of transient current pulses appearing at each device terminal.

2.2 Radiation damage

In [7], the effects of bulk radiation-damage were taken into account, to some approximated extent, by modulating the "effective doping" concentration. Such an approach, however, suffers from critical limitations: *i)* it is not appropriate for the description of non-depleted regions, and *ii)* it cannot be easily correlated to the radiation fluence (at least not in a straightforward fashion).

In the present work, a more physically-sound approach has been followed: to this purpose, the formulation of the net recombination term in Eqs. 2 and 3 has been generalized, incorporating the contribution $(G - R)_{deep}$, which accounts for the deep-level carrier traps induced by the radiation. A detailed discussion of physical mechanisms of damage and of defect kinetics goes far beyond the scope of this paper: here we shall content ourselves with a brief illustration of the implemented model, which slightly extends that presented in [8].

The model is based on a generalized Shockley-Read-Hall expression, which is applied to the case of multiple trap-levels, located deep into the bandgap. Both acceptor- and donor-type levels can be considered, and arbitrary

defect-concentrations can be assigned to each level. Levels are characterized by a set of independent parameters; namely, each level is described by the trap energy level, by the capture cross-sections for both electron and holes, and by the defect spatial density. The latter, in turn, can be correlated to the particle fluence experienced by the detector via the formulation of an introduction rate.

All of these parameters can be extracted from measurements, by means of DLTS (Deep-Level Transient Spectroscopy), TSC (Thermally Stimulated Current) or TCT (Time-resolved Current Transients) techniques [9, 10]. A quite articulated distribution of data can indeed be extracted from the literature, related to neutron- or proton-induced trap-energy levels: however, some non-negligible discrepancies can be observed between published data, and a number of details of such a distribution are not yet completely interpreted. Consequently, no unique determination of main energy levels (and parameters thereof) involved in the damage process can be reliably assumed; parameter calibration might be necessary with respect to the specific technology at hand.

A further point which should deserve deeper investigation is the correlation between the particle fluence suffered by the detector and the amount of fixed charge trapped at the oxide: in the following an empirical relationship, extracted from literature data, has been used to this purpose.

The combination of features described above makes the present version of HFIELDS a fairly powerful and versatile simulation environment for the analysis of irradiated silicon detectors: from the computational point of view, the introduction of the particle-tracking model and of the radiation damage models actually induces a negligible overhead, with respect to conventional device simulation technique.

In particular, with respect to the approach based on the effective doping concept, a more accurate physical picture, which relies on fundamentals parameters and does not suffer from basic limitations, can be achieved at no additional computational cost.

3 Simulation results

The structure sketched in Fig. 1 has been simulated. It represents a partial cross-section of an actual microstrip detector, potential candidate for CMS experiment at the future Large Hadron Collider. It consists of a *n*-type

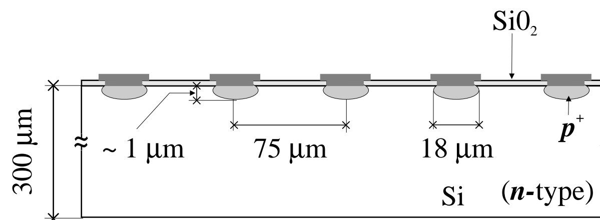

Figure 1: Cross-sectional sketch of the simulated structure.

substrate, featuring a bulk doping concentration of $8.8 \times 10^{11} cm^{-3}$. For simulation purposes, five strips have been considered, with a spacing of 75 μm. The p^+ implant ($N_A = 10^{18}\ cm^{-3}$) is 18 μm wide and 1 μm deep, whereas the metal strip width is 14 μm. An n^+ layer ($N_D = 10^{18}\ cm^{-3}$) is located at the backside ohmic-contact.

First, the non-damaged device has been simulated: an AC analysis has been carried out, aimed at extracting device capacitances. In Fig. 2 the main components of such a capacitance are reported, and compared with actual measurements, performed on a 5.5 cm long detector. Capacitance of the microstrip have been measured by using a Keithley CV 590 high precision capacimeter, whereas strip biases were supplied by highly-stable voltage sources. A positive voltage was applied to the ohmic side, with the strips on the junction-side grounded. A 100 kHz, 15 mV (RMS) AC stimulus was adopted: by injecting the signal at backplane and analyzing the strip response the backplane capacitance component was extracted; interstrip components was estimated by injecting the signal at one strip and reading the neighboring ones. Strips not involved in the actual measure were kept grounded, to minimize their influence. An identical setup was defined for the simulation. The agreement is quite satisfactory, for both the interstrip capacitances (to first- and second-neighboring strips), and for the capacitance to the backplane. It is worth observing, to this regard, that the charge trapped in the oxide and at the interface significantly affects the capacitance values, and especially the interstrip ones. A $1 \times 10^{11} cm^{-2}$ interface charge has been inferred from experiments, and has been accounted for by the simulation.

Then, in order to calibrate the damage model, we have simulated just a single-strip subset of the device. A single-level radiation-damage model, which makes such a calibration process easier, has been used in this case. Fig. 3

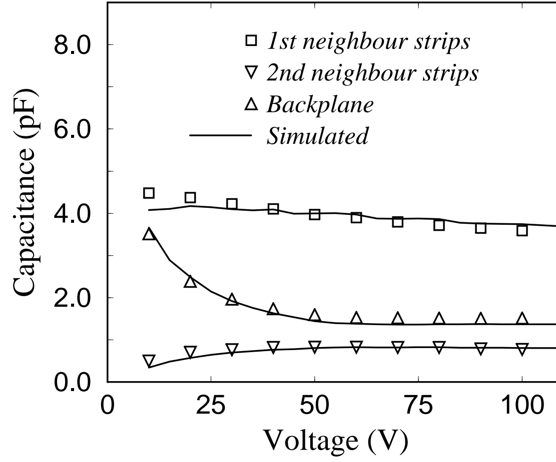

Figure 2: Non-irradiated device capacitances.

shows the behavior of the predicted effective doping concentration (i.e., the absolute value of space-charge density) as a function of the radiation fluence. Depending on the trap energy level, three curves are reported, the minima of

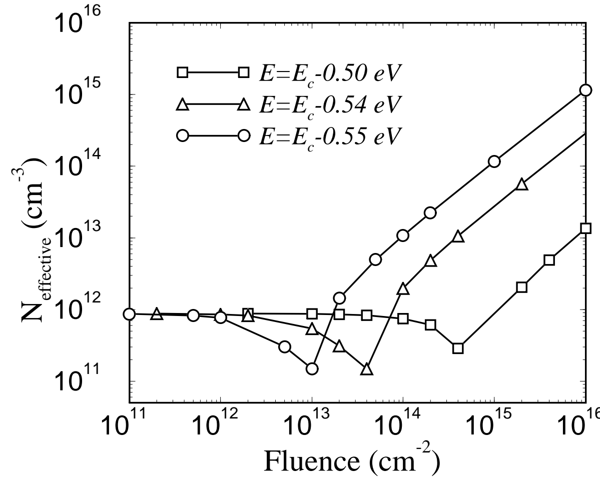

Figure 3: Effective doping concentration vs. radiation fluence.

which indicate the inversion point, i.e., the fluence at which the n-substrate effectively turns into a p one. For the device under study (having an initial resistivity of about 5 kΩ·cm), inversion is expected to occur at $1 \times 10^{13} cm^{-2}$ fluence, which corresponds to a single level located slightly above the midgap ($E = E_c - 0.55eV$).

At this point, we were able to repeat the comparison on the capacitance components for heavily irradiated devices. In particular, a fluence of $1 \times 10^{14} cm^{-2}$ neutrons has been accounted for by the simulations, corresponding to several years of real operation at LHC. Measures were instead carried out on some detectors, purposely irradiated with neutrons (the mean-energy of which was $\sim$1 MeV) at the nuclear reactor of the ENEA facility in Rome. The comparison is illustrated by Fig. 4: an overall satisfactory agreement is still retained, even if larger discrepancies are found in this case, with respect to the non-irradiated device. Such discrepancies are less evident in the operative, high-voltage range; they are likely to be due to some uncertainty in the determination of some parameters, and, in particular, of the amount of extra-charge trapped at the interface and induced by the radiation. In this case, in fact, no measure has been done, and a tentative value was extrapolated from literature works.

Among the relevant design issues, the depletion voltage can be extracted from the backplane capacitance plot shown in Fig. 4, and thus correlated to the radiation suffered by the device. Simulations have been carried out at different fluences: the predicted depletion voltages are collected in Fig. 5, and compared with a few measured data. The shape of the curve well compares also with literature data (see, e.g., [11]), the minimum of such a curve again

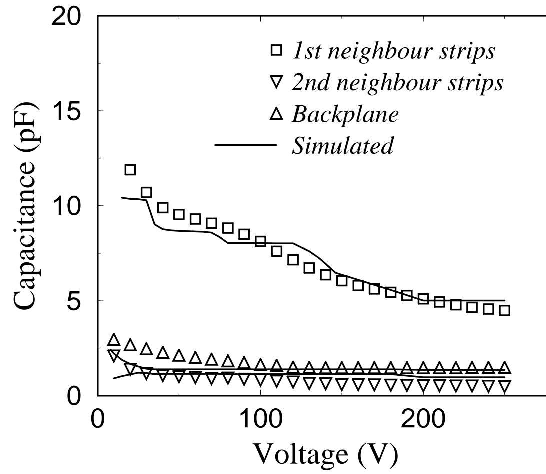

Figure 4: Irradiated device capacitances ($\Phi = 1 \times 10^{14} n \cdot cm^{-2}$).

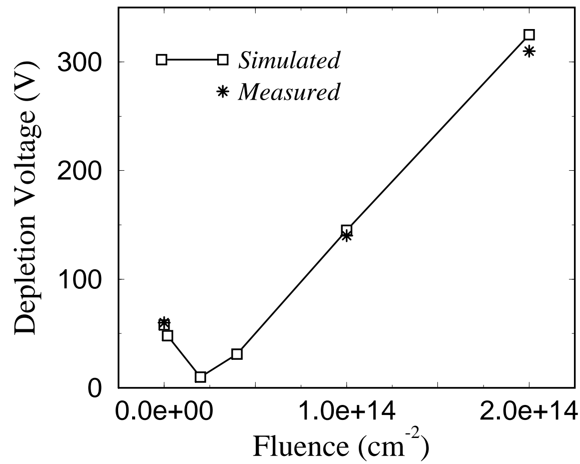

Figure 5: Depletion voltage vs. particle fluence.

indicating the aforementioned type-inversion fluence.

Another important performance indicator is the leakage current, which is expected to increase linearly with the defect concentration. Such a qualitative behavior is correctly predicted by the simulation, as shown in Fig. 6. From this plot, a damage constant $\alpha = 2.2 \times 10^{-18} Acm^{-1}$ can be inferred. Such a value is slightly lower than expected: a similar underestimate is actually reported and discussed in [12]. Schenk and Krumbein [13] suggest such an effect to be possibly due to an efficient inter-center transition mechanism, i.e., inter-level charge transfer not assisted by the valence or conduction band. The model adopted here, however, assumes a single deep level and is therefore inherently not able to account for such a phenomenon.

In the following, results of transient simulations are illustrated, discussing the active behavior of the detector. A single particle crossing the device is accounted for, which hits the detector at the middle of a strip. Currents collected by the strip are plotted in Fig. 7, as predicted for different fluences. As mentioned above, when the fluence exceeds the type-inversion point, the full depletion occurs at higher bias voltages and an increasing amount of carriers populates the bulk. This is made more evident by Figs. 8, which shows the hole concentration calculated within the device, for three different fluence values. Mobile charge concentration increases with fluence, eventually resulting in a partial depletion only (Fig. 8.c). A charge collection efficiency can be defined, as the ratio between the total amount of charge actually collected by the strip, and the charge that it would have been collected by the non-irradiated device. Fig. 9 report such an efficiency, as calculated by integrating the strip current pulses. The prediction well agrees with the experimental finding, as well as with more complete discussion find in the literature

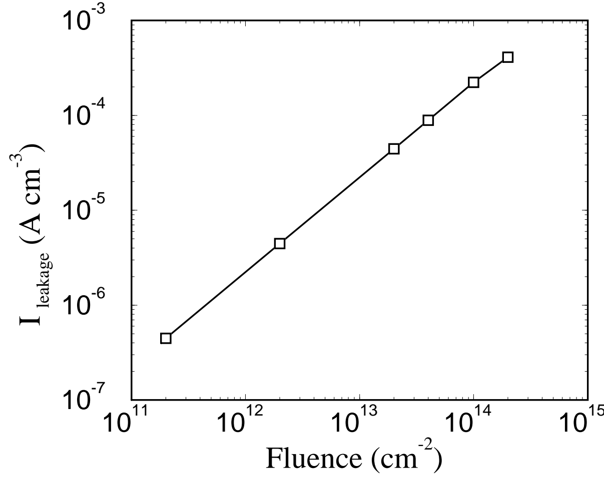

Figure 6: Leakage current (per unit volume) vs. particle fluence.

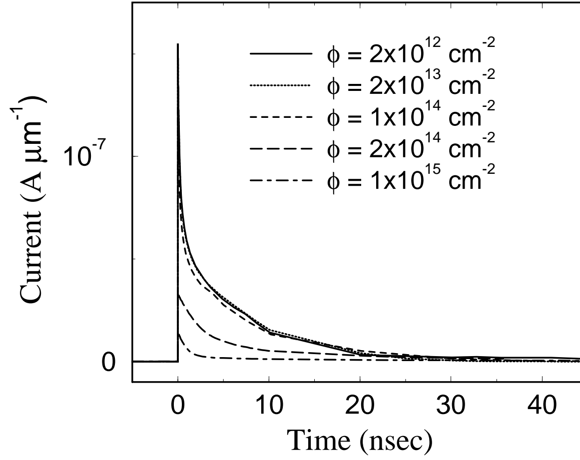

Figure 7: Time-domain responses to a single-particle hit (V_{bias} = $250V$).

[14].

Simulation results shown, up to this point, fit in a rather satisfactory way the actual device performances, and demonstrate the potential usefulness and practicality of TCAD tools for detector design. However, such results have been obtained by using a somehow simplified model, based on single energy-level trapping mechanisms. The actual physical picture is known to be more complex: to appreciate this point, in the remaining part of this section, we shall try to address a few issues, by looking at some preliminary results obtained with more sophisticated models. In particular, we used a two-level model, including an acceptor level located at $E = E_c - 0.42eV$ and a donor one, located at $E = E_v + 0.36eV$. The level parameters are independently defined: since the experimental characterization of such parameters exceeds the scope of this work, we assumed values referenced in the literature [9] and performed no fitting procedure. I.e., no attempt has been made to tune the two-level model with respect to the single-level one. In the following, we shall therefore limit ourselves to mostly qualitative considerations

Fig. 10 shows the equilibrium bulk carrier concentration, depending on the particle fluence experienced, as predicted by the single-level model used for the previous discussion. The plot also shows the amount of charge trapped at such a deep acceptor level: it appears how at high fluences (i.e., at high defect concentration) the dominant contribution to hole generation comes from the deep level itself. If two levels (one acceptor and one donor) are assumed instead, a significantly different situation is predicted, as illustrated in Fig. 11. Although direct, inter-level transitions are neglected in this case as well, a statistical compensation between the levels is evident nevertheless: beyond a certain fluence, and if introduction rates for the two levels do not appreciably differ, acceptor and donor

levels reciprocally annihilate, and the mobile charge concentrations “saturate” at a much lower level than the defect concentration. The two approaches may therefore lead to drastically different estimates for the carrier concentration, which in turn reflect on the simulated performance. However, such discrepancies become sensible in the very high fluences range, this possibly justifying the adoption of the simplest model for moderate fluences.

Another point which deserves some attention is illustrated by Figs. 12 and 13. Here, the hole concentration profile along the vertical direction (i.e., normal to the detector surface) is shown, for different values of the applied bias. Most of the interpretative models of the detector behavior rely on the assumption of a one-sided junction structure. For non-irradiated or weakly irradiated structures (not shown in figures), the space-charge region develops starting from the junction side, whereas, after the inversion fluence, the effective junction is at the ohmic side, so that the space charge region is expected to move from such a side toward the strips. This is actually predicted by the single-level model, as shown in Fig. 12.

Some authors [15, 16], however, report about the evidence of a double-sided depletion mechanism, which can be appreciated if the two-level model is accounted for (Fig. 13). This is consistent with the different carrier concentrations (after inversion) illustrated in Figs. 10 and 11: for a given defect concentration, charge densities differ significantly, and so do the electrostatic potential profiles. Further investigations are needed to explain details of such a mechanism: the donor level plays indeed a role in modifying the spatial distribution of trapped charge, which could be responsible for this behavior.

These results may critically affect the estimate of the charge collection efficiency, which is sensitive to the spatial distribution of charge; in the limit case, at very large fluences detectors may happen to operate in partial depletion conditions. Under these circumstances, the undepleted region may act as an absorbing layer for the excess charge: its actual position clearly determines the collection dynamics.

4 Conclusions

In this work, numerical simulation techniques are presented, aimed at providing suitable means for the analysis of solid-state, silicon detectors used in high-energy physics. In particular, a fully-featured, general purpose device simulator has been customized by incorporating numerical and physical models for both the impinging radiation and the radiation damage. A set of simulation results have been discussed and compared with actual device measurements. Experimental data have been closely matched by using a single deep-level trap model. Intrinsic limitations of such a model have also been discussed, by comparison with a two-level one. Qualitative differences have been illustrated, which are expected to become more significant at large radiation fluences. In particular, evidence of a double-sided depletion mechanism has been predicted. The introduced features, therefore, allow for building up a simulation environment suitable for the versatile and accurate analysis of radiation-sensitive devices: detector designers may evaluate radiation hardness in a fast and inexpensive way, as well as gain physical insight on many operating details which are hard to investigate experimentally.

5 Acknowledgements

The authors gratefully acknowledge the contribution of Prof. M. Rudan and Dr. M. Valdinoci, from the University of Bologna, Italy, and of Dr. L. Colalongo, from the University of Trento, Italy, who developed the original code for the generalized SRH treatment.

References

[1] P. Ciampolini, A. Pierantoni, M. C. Vecchi and M. Rudan, “Application of a general-purpose device simulator to the analysis of integrated silicon microsensors,” *Sensors and Materials*, vol. 6, n. 3, pp. 139-157, 1994.

[2] R. Della Marina, D. Passeri, P. Ciampolini and G.M. Bilei, “Silicon Strips Detectors for LHC: comprehensive process and device analysis,” *4th International Conference on Position Sensitive Detectors,* Manchester, 1996.

[3] B.C. MacEvoy, “Defect kinetics in silicon detector material for applications at the Large Hadron Collider,” Ph. D. Thesis, RAL-TH-97-003, Imperial College, London, 1997.

[4] J. Matheson, M.S. Robbins and S.J. Watts, “The effect of radiation induced defects on the performance of high resistivity silicon diodes,” CERN RD20 Technical Report TN/36, 1995.

[5] E.H. Nicollian and J.R. Brews, “Radiation effect in $Si0_2$,” *MOS Physics and Technology*, Wiley, 1981.

[6] G. Baccarani, P. Ciampolini and A. Pierantoni, “Three-dimensional simulation of semiconductor devices: state of the art and prospects,” *Nucl. Instr. and Meth.,* vol. A326, pp. 253-259, 1993.

[7] D. Passeri, P. Ciampolini, M. Baroncini, A. Santocchia, G.M. Bilei, B. Checcucci and E. Fiandrini, “Comprehensive Modeling of Silicon Microstrip Detectors,” *IEEE Trans. on Nucl. Sc.,* vol. 44, n. 3, pp. 598-605 , 1997.

[8] Marina Valdinoci, Luigi Colalongo, Aurelio Pellegrini and Massimo Rudan, “Analysis of Conductivity Degradation in Gold/Platinum-Doped Silicon,” *IEEE Trans. on Electron Devices*, vol. 43, n. 12, pp. 2269-2275, 1996.

[9] H.W. Kraner, Z. Li and E. Fretwurst, “The use of the signal current pulse shape to study the internal electric field profile and trapping effects in neutron damaged silicon detectors”, *Nucl. Instr. and Meth.,* vol. A326, pp. 350-356, 1993.

[10] E. Fretwurst, V. Eremin, H. Feick, J. Gerhardt, Z. Li and G. Lindstrom, “Investigation of Damage Induced Defects in Silicon by TCT,” HH/96-03 Technical report, 1996.

[11] S.J. Bates, B. Dezillie, C. Furetta, M. Glaser, F. Lemeilleur, “Proton irradiation of silicon detectors with different resistivities,” *IEEE Trans. on Nucl. Sc.,* vol. 43, n. 3, p. 199, 1996.

[12] S.J. Watts, J. Matheson, I.H. Hopkins-Bond, A. Holmes-Siedle, A. Mohammaddzadeh, and R. Pace, “A new model for generation-recombination in silicon depletion regions after neutron irradiation,” CERN ROSE/TN/96-2 Technical Report, 1996.

[13] A. Schenk and U. Krumbein, “Coupled defect-level recombination: theory and application to anomalous diode characteristics,” J. of Appl. Phys., Vol. 78, n. 5, pp. 3185-3192, 1995.

[14] C. Leroy, M. Glaser, E.H.M. Heijne, P. Jarron, F. Lemeilleur, J. Rioux, C. Soave, I. Trigger, “Study of the electrical properties and charge collection of silicon detectors under neutron, proton and gamma irradiations,” *Proc. of IV Int. Conf. on Calorimetry in High-Energy Physics,* La Biodola, Italy, 1993.

[15] V. Eremin, Z. Li and I. Iljashenko, “Trapping induced N_{eff} and electrical field transformation at different temperatures in neutron irradiated high resistivity silicon detectors,” *Nucl. Instr. and Meth.,* vol. A360, pp. 458-462, 1995.

[16] M. Bosetti, C. Furetta, C. Leroy, S. Pensotti, P.G. Rancoita, M. Rattaggi, M. Redaelli, M. Rizzatti, A. Seidman and G. Terzi, “Effect on charge collection and structure of n-type silicon detectors irradiated with large fluences of fast neutrons,” *Nucl. Instr. and Meth.,* vol. A343, pp. 435-440, 1994.

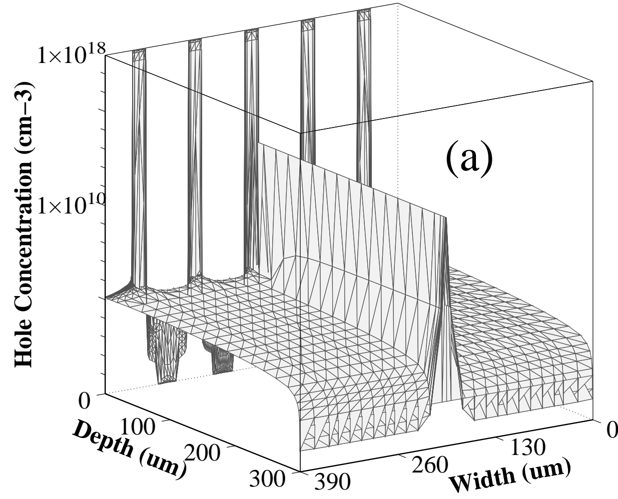

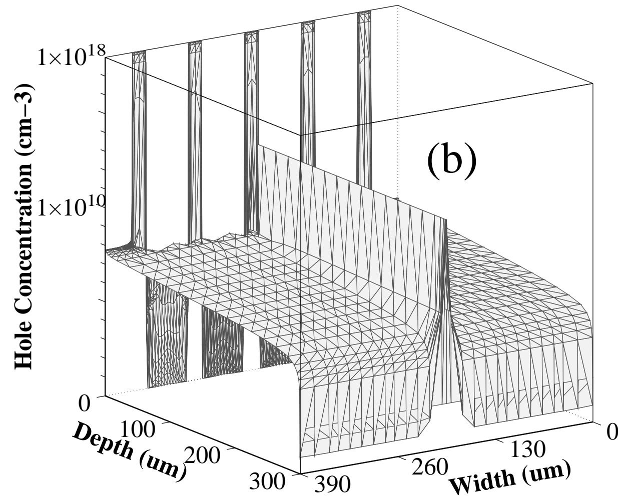

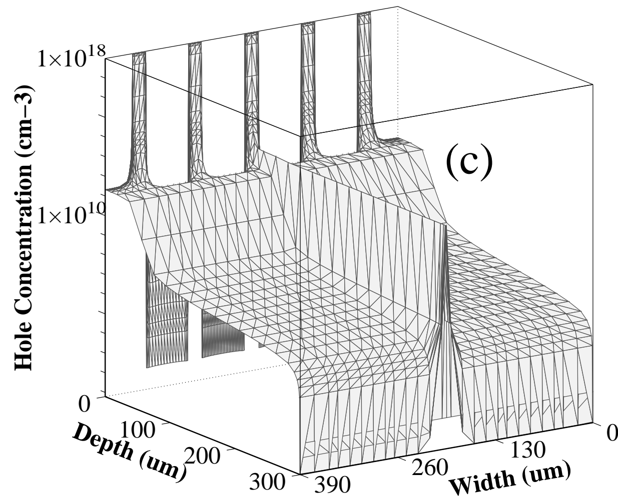

Figure 8: Hole distribution, just after the particle hit, for different fluences (a: non irradiated, b: $\Phi = 1 \times 10^{14} n \cdot cm^{-2}$, c: $\Phi = 2 \times 10^{14} n \cdot cm^{-2}$; $V_{bias} = 250V$) .

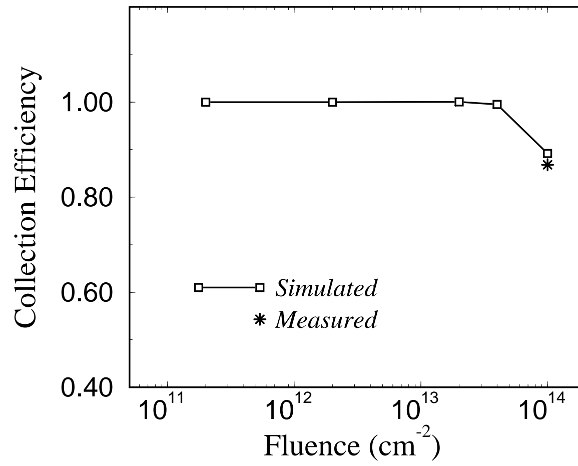

Figure 9: Charge collection efficiency vs. fluence ($V_{bias} = 250V$).

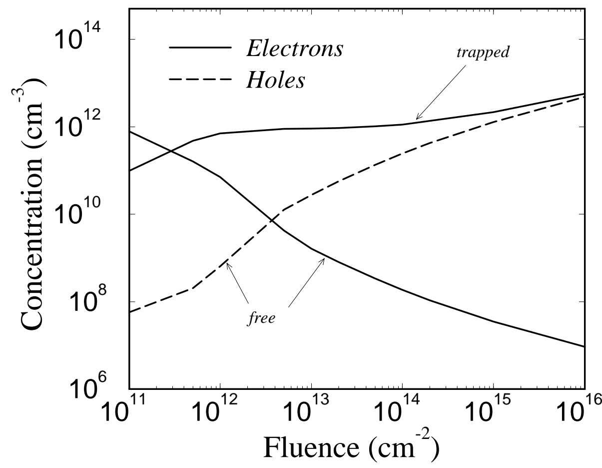

Figure 10: Equilibrium carrier concentration vs. fluence: single level model.

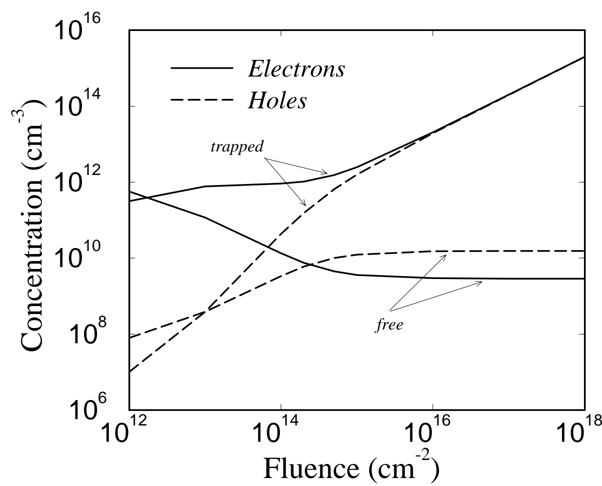

Figure 11: Equilibrium carrier concentration vs. fluence: two-level model.

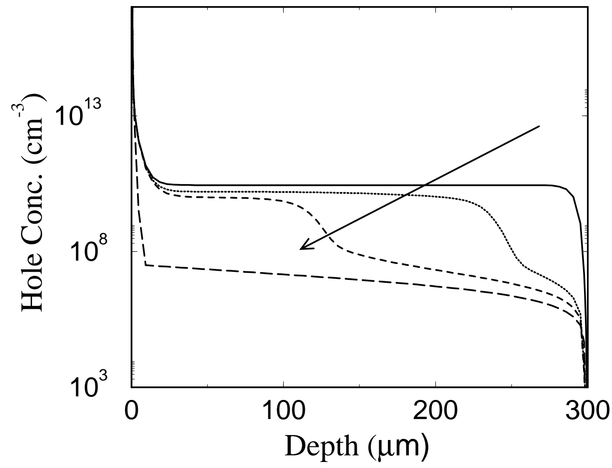

Figure 12: Space charge region build-up: single-level model prediction. The arrow indicates the concentration profiles obtained for increasing bias voltages: V_{bias} =0, 1, 7.5, 40 V, respectively.

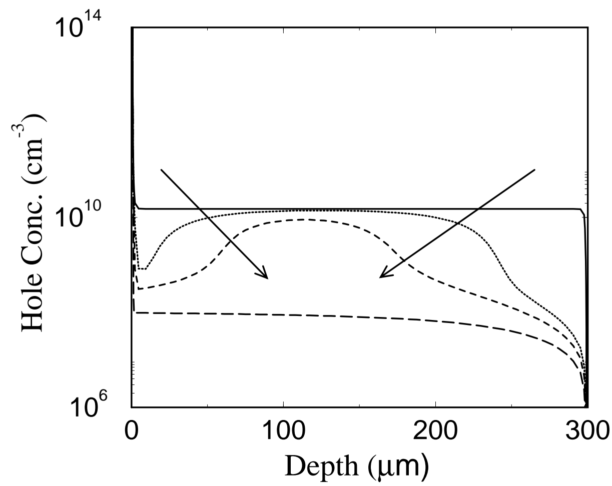

Figure 13: Space charge region build-up: two-level model prediction. The arrows indicate the concentration profiles obtained for increasing bias voltages: V_{bias} =0, 2.5, 10, 80 V, respectively.